Polymer 300 (2024) 126982

Contents lists available at ScienceDirect

Polymer

journal homepage: www.elsevier.com/locate/polymer

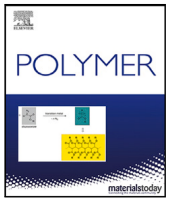

Elucidation of smear wear layer structure and ageing mechanisms of filled tyre tread compounds

E. Koliolios [a], S. Nakano [b], T. Kawamura [b], J.J.C. Busfield [a,*]

[a] School of Engineering and Materials Science, Queen Mary University of London, Mile End Road, London, E1 4NS, United Kingdom
[b] Sumitomo Rubber Industries, Ltd, Kobe, Japan

ARTICLE INFO

Keywords:
Tyre tread wear
Smear wear
Dynamic mechanical analysis
Microstructural investigation
Material characterisation

ABSTRACT

This paper explores the microstructure of smear wear particles generated during the abrasion of tyre tread compounds made from different polymers. The compounds tested were synthetic polyisoprene rubber (IR) and styrene-butadiene rubber (SBR) reinforced with either carbon black or silica. This study used a range of different experimental techniques including Gel Permeation Chromatography (GPC), Dynamic Mechanical Analysis (DMA Rheology), Thermal Gravimetric Analysis (TGA) and Scanning Electron Microscopy (SEM) on both fresh and aged smear wear particles to understand their structure and ageing mechanisms. This research reveals that there is significant difference between the molecular weights of the initial uncured rubber and smear wear particles. Significant differences are also observed in the filler volume fraction and the nature of polymer filler interaction between the cured rubber and smear wear particles generated from abrasion. The results also reveal a second relaxation process in smear wear particles, which is attributed to decrosslinked polymer content. After comparing the ageing effect of 1 day and 1 month to smear wear particle properties it was also discovered that the ageing mechanisms are dominated by the recovery of the filler network in the short term and by oxidation-driven crosslinking in the polymer over the longer time frame. The microstructure of the smear wear particles proposed from these results is confirmed by a detailed investigation using SEM techniques.

1. Introduction

Rubber wear is commonly described using three different mechanisms: Abrasive Wear, Smear Wear and Fatigue Wear. Abrasive and Fatigue wear have been studied extensively in the literature [1–5]. The concepts of these types of mechanical and thermo-mechanical wear have been well understood and modelled, however chemical wear in the form of smear wear has not yet been analysed to the same extent and the mechanisms of its formation are not yet fully understood. Gent and Pulford [3] investigated smear wear and described it as an oxidative mechanism. Ahagon [6] further investigated these oxidative mechanisms which lead to the chemical degradation of rubber and smear wear phenomenon. Nakano et al. [7] confirmed that the formation of smear wear is an oxidative phenomenon, by conducting an abrasion experiment in an oxygen free atmosphere. This lead to the production of a powdery substance while the same compound abraded under the same conditions produced smear wear in air. Wu et al. [8,9] investigated and characterised smear wear and its production through blade abrasion, however no in depth discussion regarding the microstructure of smear wear particles which were generated, was performed. One of the observations from Wu et al.'s [9] work was that the smearing material has a significant amount of decrosslinked polymer content. Additionally, Wu et al. [9] also reported that the solubility of smear wear particles in toluene changed significantly over the first 24 h, since the fresh samples were soluble whereas the samples aged for 24 h became insoluble. The enhanced solubility of smear wear particles was also reported by Huang et al. [10]. These two observations along with studies performed by Tsagaropoulos and Eisenberg [11] and later by Robertson and Rackaitis [12], where there has been extensive discussion regarding an un-crosslinked polymer phase which creates a second relaxation of the tanδ are important indications that more detailed research is still required to fully understand this. Therefore, this study examines the microstructure of smear wear particles to understand the process of its formation and its ageing mechanisms by experimenting on 6 widely different tyre tread compounds, with a range of different fillers and polymers.

* Corresponding author.
E-mail address: j.busfield@qmul.ac.uk (J.J.C. Busfield).

https://doi.org/10.1016/j.polymer.2024.126982
Received 28 November 2023; Received in revised form 4 March 2024; Accepted 25 March 2024
Available online 28 March 2024

Table 1
Final formulation of IR tyre tread compounds.

Components	IRN220 (phr)	IRVN3 (phr)
IR (Nipol IR2200)	100	100
N220 (with a Specific Surface Area of 106 m^2/g)	70	5
Ultrasil VN3 (with a Specific Surface Area of 180 m^2/g)	–	65
Wax	1.5	1.5
6PPD	2	2
TMQ	0.8	0.8
Stearic Acid	2	2
Zinc Oxide	2	2
Process Oil	22	22
Sulphur	1.7	1.4
TBBS	2.0	2.0
DPG	–	2.0
Si266	–	6.5

Table 2
Final Formulation of SBR tyre tread compounds.

Components	SBRN220 (phr)	SBRVN3 (phr)	SBRN134 (phr)	SBR9100GR (phr)
SBR (NS522)	137.5	137.5	137.5	137.5
N220 (with a Specific Surface Area of 106 m^2/g)	70	5	–	5
N134 (with a Specific Surface Area of 137 m^2/g)	–	–	70	–
Ultrasil VN3 (with a Specific Surface Area of 180 m^2/g)	–	65	–	–
Ultrasil 9100GR (with a Specific Surface Area of 235 m^2/g)	–	–	–	65
Wax	1.5	1.5	1.5	1.5
6PPD	2	2	2	2
TMQ	0.8	0.8	0.8	0.8
Stearic Acid	2	2	2	2
Zinc Oxide	2	2	2	2
Process Oil	–	–	7	7
Sulphur	1.7	1.45	1.7	1.45
CBS	2.2	2.2	2.2	2.2
DPG	–	2.2	–	2.4
Si266	–	5.2	–	6.5

2. Materials and methods

2.1. Materials

Two IR and four SBR compounds were selected for this investigation. The IR compounds were filled with carbon black (CB) and silica respectively. Their formulation is presented in Table 1. Two of the SBR compounds were filled with CB of different colloidal properties and two of the SBR compounds were filled with silica with different colloidal properties. The formulation of the compounds is presented in Table 2. The total filler loading in all six elastomer compounds was controlled at 70 parts per hundred rubber (phr). The SBR selected for the compounds was produced through oil extended solution polymerisation. There are 37.5 parts of oil for every 100 parts of SBR. The compounds were supplied by Sumitomo Rubber Industries, Ltd. The compounds were cured after obtaining the time required for the compound to reach 90% of its maximum torque value (t_{90}) which was calculated using a MDR2000 Moving Die Rheometer (MDR) from Alpha Technologies. The compounds were cured at 160 ° C using a hot press at t_{90} + 13 min, an empirical practice to compensate for the thickness of the discs which were 13 mm thick. The values of t_{90} of the compounds investigated, along with the curing times for each disc of each compound are provided in Table 3.

Table 3
Optimal Curing Time for the compounds of interest at 160 °C.

Compound	t_{90}/min	Actual Curing Time/min
IRN220	6.81	19.81
IRVN3	8.72	21.72
SBRN220	12.38	25.38
SBRVN3	11.39	26.39
SBRN134	11.75	26.75
SBR9100GR	13.04	28.04

2.2. Methods

2.2.1. Blade abrasion

The blade abrasion test was performed using a purpose built blade abrasion machine, to simulate real-world smear wear conditions by inducing smearing artificially. The blade abrasion machine setup is shown in Fig. 1. The machine rotates a rubber disc through a driving motor. The motor rotates a disc whose diameter can be changed to create different rotational speeds, which in turn rotates the rubber disc which is abraded by a blade. Dead weights are placed on top of the blade to create a normal force and a damper filled with oil is installed to avoid excessive vibrations. The rubber discs were abraded at a rotational speed of 75rpm and a normal load of 10N for 30 min. Smear wear particles were collected from the surface of the disc using VWR Superfrost Plus microscope adhesion slides. The slides were held underneath the rotating disc and by applying a force by hand on the disc using the slide, smear wear particles were deposited on its surface as shown in Fig. 2. The average room temperature during the abrasion experiments was 21.85 °C with a standard deviation of 0.32 °C and respectively the average humidity was 30.4% with a standard deviation of 3.6%. All the compounds discussed in this research produced smear wear particles during blade abrasion under the conditions tested .

2.2.2. Gel permeation chromatography (GPC)

An Agilent 1260 Infinity system GPC was used to measure the molecular weight distribution of the uncured rubber compounds and the smear wear particles. A minimum of 10 mg of rubber was dissolved in tetrahydrofuran (THF) for 48 h. The resulting solutions were filtered through a 0.2 μm polytetrafluoroethylene syringe filter and then GPC runs were performed with a constant flow rate of 1 mL/min for 40 min.

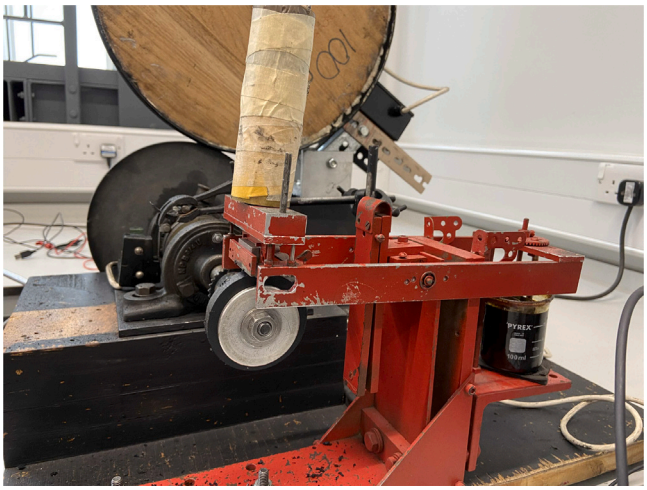

Fig. 1. Blade abrasion machine used for the production of smear wear particles.

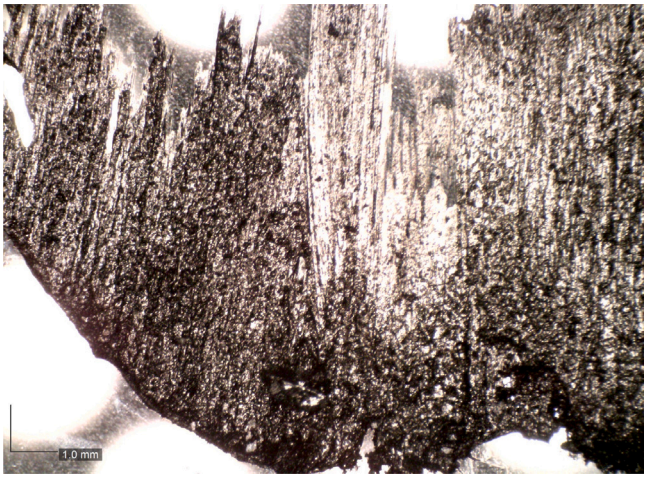

Fig. 2. Smear wear particles collected on glass slide.

The GPC is equipped with Refractive Index Detector (RID), 2 PLgel 5 μm mixed-C columns (300 mm *x* 7.5 mm), a PLgel 5 mm guard column (50 mm *x* 7.5 mm) and an autosampler. The columns and the RID were operated at 40 °C. The instrument was calibrated with linear narrow poly(methyl methacrylate) standards in a range of 550 to 2136000 g/mol.

2.2.3. Thermogravimetric analysis (TGA)

Thermogravimetric Analysis was performed using a TA Instruments TGA 5500. The samples were placed in high temperature platinum pans and were ramped up from room temperature to 800 °C at a heating rate of 10 °C/min in a nitrogen environment. When the final temperature of 800 °C was reached, the environment was switched to air for 5 min to burn any residual carbon material.

2.2.4. Dynamic mechanical analysis

A TA Instruments Discovery HR-3 hybrid rheometer was used to evaluate the dynamic mechanical properties of the smear wear particles, in shear mode, generated during blade abrasion performed at 75rpm and 10N and collected after 30 min. The rheometer was fitted with a Peltier plate and an 8 mm diameter shaft. Strain sweeps were performed at ambient temperature (20 °C) and at an oscillation frequency of 10 Hz between 0.1% and 50% oscillation strain, using a pre-load of 9.0N for smear samples of each compound. Temperature

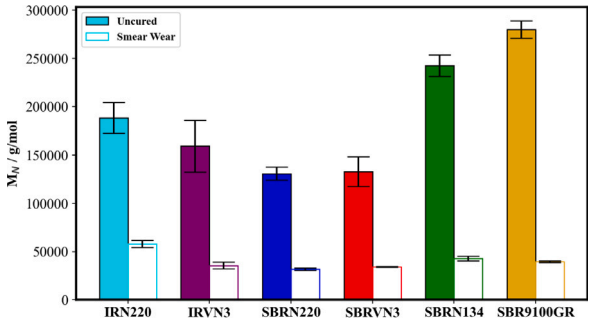

Fig. 3. Number average molecular weight of uncured compounds and the smear wear particles generated.

sweeps were performed at an oscillation strain of 0.2% and an oscillation frequency of 10 Hz between 0 °C and 140 °C, using a pre-load of 9.0N for smear samples of each compound. Approximately 5mg of smear wear particles were transported from the glass slides on to the Peltier plate using forceps and a scalpel to form compact test sample. Due to their strong, natural adhesive properties, smear wear layer samples adhered to the Peltier plate, the rheometer shaft was then brought in to contact with the sample and a pre-load of 9.0N was applied, and thus slippage was prevented during the experiment. Smear wear layer samples were tested immediately after their production, however some samples were left to age inside a Petri dish at ambient temperature for either 24 h or 1 month to investigate the evolution of the smear wear particle properties. The 24 h ageing scenario corresponds to short term ageing, which might have implications to tyre performance and wear. The 1 month ageing scenario corresponds to long term ageing, which might have implications to the behaviour and decomposition time of smear wear particle debris in the environment.

2.2.5. Scanning electron microscopy (SEM)

A FEI Inspect-F Scanning Electron Microscope was used to examine the microstructure of smear wear particles formed during blade abrasion. The examined smear wear layer samples were produced the same day the experiment was conducted and were coated with a gold layer before SEM was performed.

3. Results

3.1. Investigating smear wear particle structure through GPC

Understanding the polymer structure of the smear wear particles is extremely important, as it helps to explain its properties. The comparison of the number average molecular weight of smear wear particles and the original uncured compound could therefore be an important technique to help further our current understanding of smear wear particles.

As presented in Fig. 3, the smear wear particles number average molecular weight is significantly smaller than the uncured compound. This confirms that chain scission and oxidation during abrasion creates a significant reduction in polymer chain length.

To further quantify chain scission, the percentage difference between the number average molecular weight of uncured samples, $M_{uncured}$ and smear wear layer samples, M_{smear}, is defined as $(M_N)_{\%diff}$ and it is calculated using the following equation:

$$(M_N)_{\%diff} = 100 \times \left(\frac{M_{uncured} - M_{smear}}{M_{uncured}}\right)_N \quad (1)$$

From Fig. 4, there is an apparent difference between the six different compounds. SBR9100GR and SBRN134 appear to have the largest $(M_N)_{\%diff}$ values whereas the two smallest values are attained by IRN220 and SBRN220, which are both filled with CB N220. A higher

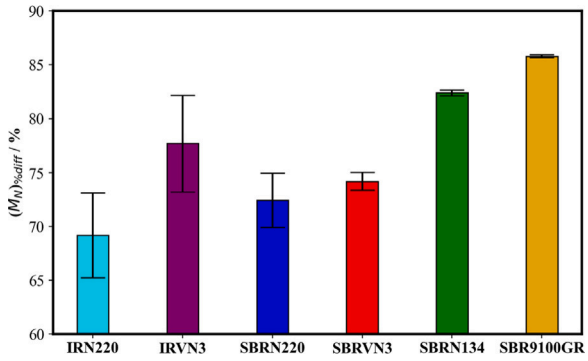

Fig. 4. Number average molecular weight percentage difference between uncured compounds and the smear wear particles generated.

value of $(M_N)_{\%diff}$ suggests that a more significant amount of backbone damage occurred in the polymer chain during abrasion. Therefore, as SBR9100GR and SBRN134 appear to have the most significant amount of backbone damage it is likely that there are more radicals generated in these compounds. A higher amount of radicals generated results in more rapid rate of smear wear particle generation and a larger susceptibility to chain scission and oxidation in these two compounds. SBR91000GR and SBRN134 are also the compounds with the highest specific surface area silica and carbon black particles respectively, thus the polymer-filler interactions appear to play an important role, as damage to the polymer filler interface might also generate free radicals which boost molecular weight reduction and smear wear particle generation.

3.2. Investigating smear wear particle structure through TGA

Investigating the difference between smear wear layer samples and cured rubber using TGA was undertaken to understand the polymer and filler content and also their structure. The TGA weight loss in nitrogen up to 800 °C of IRVN3 and SBRVN3 is shown in Fig. 5. It appears that the smear wear layer samples have a lower decomposition temperature compared to the cured rubber samples, since the molecular weight is significantly smaller in smear wear layer samples, as was previously discussed by Wu et al. [9]. After 800 °C was reached, the atmosphere was switched to air and an isothermal process was performed for 5 min to approximate the residual CB and ash/silica contents of the samples. The methodology used to calculate the content of the samples by percentage and generate Table 4 is presented in Figure 22 in the Supplementary Material section From Table 4, there seems to be rather insignificant difference regarding the polymer and filler content change between cured and smear wear samples layer, however in the case of SBRN134 and SBR9100GR there appears to be a surprising slight increase in the CB content. The CB content of SBR9100GR increased by 4.83% and SBRN134 increased by 1.38%, implying that there are underlying mechanisms which result in higher CB content in the smear wear particles.

As mentioned in the "Investigating smear wear particle structure through GPC" section, SBRN134 and SBR9100GR were also the compounds with the highest $(M_N)_{\%diff}$, implying that more radicals are generated by these compounds during abrasion. These radicals which are created due to chain scission and oxidation during abrasion potentially stick to CB sites as proposed in Fig. 6. According to the proposed mechanism, during abrasion, the CB structure experiences strain as well as heat, which results in structure alteration and breakdown. Simultaneously, chain scission occurs locally around the CB surface and therefore low molecular weight polymer radicals are created which then attach on the CB surface. The radical scavenging function of carbon black has been initially proposed by Gruver [13] and further

Table 4
TGA Results for Cured rubber and Smear Wear particles.

Cured Rubber Samples			
Compounds	Polymer + Additives (%)	Carbon Black (%)	Silica (%)
IRN220	65.16	33.43	–
IRVN3	67.68	2.17	29.15
SBRN220	67.31	31.42	–
SBRVN3	70.18	2.80	27
SBRN134	68.37	30.06	–
SBR9100GR	70.70	2.83	26.31
Smear Wear Layer Samples			
Compounds	Polymer + Additives (%)	Carbon Black (%)	Silica (%)
IRN220	63.7	33.08	–
IRVN3	68.35	2.28	28.37
SBRN220	67.38	30.09	–
SBRVN3	70.36	4.09	25.54
SBRN134	68.84	27.13	–
SBR9100GR	68.6	7.66	23.74

discussed by Bevilacqua [14]. Additionally, the chain scission location might be of significant importance. As mentioned by Robertson and Hardman [15], the local crosslink density immediately around the CB polymer interface is larger than that of the rest of the bulk rubber due to carbon black reportedly acting as a catalyst in both polyisoprene and SBR [16,17]. Thus there is potentially a high density of chain scission around the polymer-filler interface. The high crosslink density of polymer phase around the CB has higher elastic modulus locally, therefore, a large difference of the moduli exists between the normal polymer phase and the polymer phase on the CB surface. The difference in moduli causes a high stress concentration around the surface of CB under the large deformation applied during abrasion. Such large strain and the resultant stress caused by mechanical concentration would accelerate the chain scission reaction around the surface of CB. As a result, it is proposed here that there is a higher density of chain scission around the polymer filler interface. As mentioned above, the CB acts as the radical scavenger, so the radicals generated by the chain scission reaction around the surface of CB also should be scavenged by CB, which resulted in the suppression of the polymer recombination reaction after chain scission.

To further confirm this mechanism, the TGA weight loss was plotted against heating time from the introduction of air at 800 °C for smear wear particles and cured rubber samples as presented in Fig. 7. Fig. 7(a) was constructed solely for the isothermal decomposition of the CB filled compounds and Fig. 7(b) for the isothermal decomposition of the silica filled compounds. The smear wear layer samples decompose more rapidly than the cured samples for all of the compounds, even for silica filled compounds which contained only 5phr of CB. This potentially implies that the oxygen content of the CB surface is significantly higher in smear wear particles compared to that in cured rubber.

To quantify the rate of decomposition, the slope of each graph was measured to allow a comparison that is shown in Fig. 8. Additionally, the difference between the slope of smear wear layer samples and cured samples are plotted in Fig. 9. From Fig. 9 it was observed that the higher specific surface area CB filled SBR has the highest difference in decomposition slope. Such observation can be explained by the increased amount of radicals generated as suggested by significant backbone damage observed in the GPC. Additionally, higher specific surface area carbon black particles are expected to have higher local crosslink density around them, resulting in more chain scission and more radicals. The radicals generated during this process are either absorbed or bonded to the CB surface. IRN220 also has a large difference

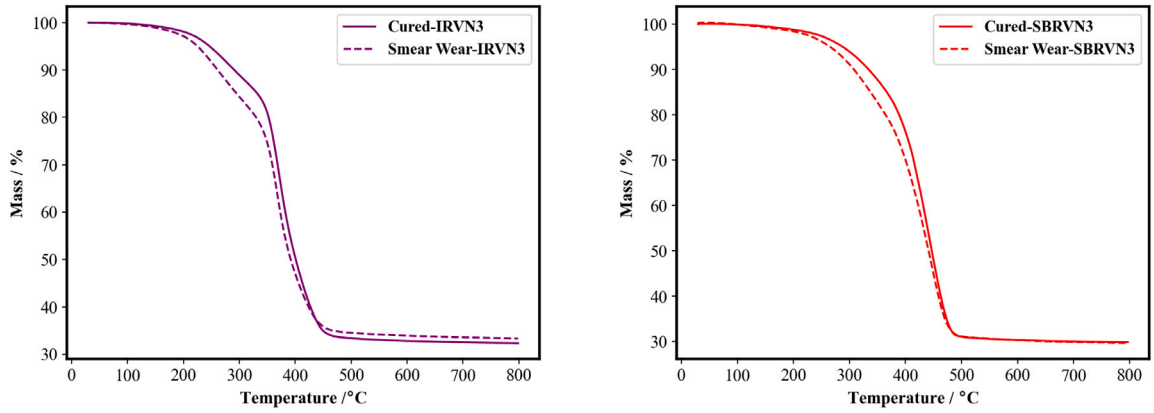

Fig. 5. TGA weight loss in nitrogen up to 800 °C of (a) IRVN3 and (b) SBRVN3.

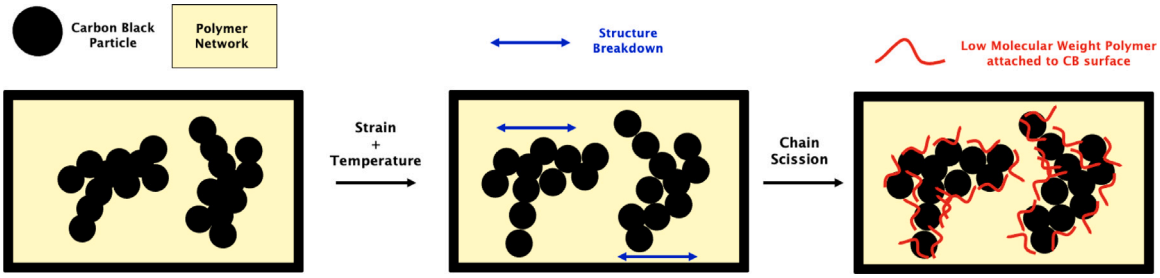

Fig. 6. Possible mechanism of polymer attaching on carbon black surface after chain scission and oxidation.

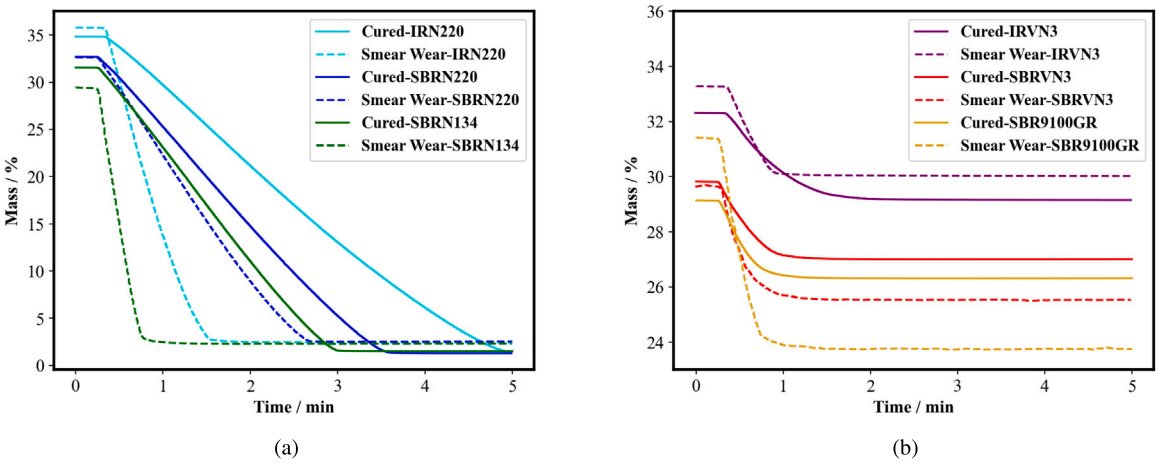

Fig. 7. TGA weight loss in air at 800 °C over a time of 5 min of (a) CB samples and (b) Silica samples.

in its decomposition slope, which is not expected according to the GPC results, however this might be due to local crosslink density around the CB surface. Comparing IRN220 and SBRN220, which both include 70phr of N220, there appears to be a large difference in the change in slope value between cured rubber and smear wear particles. Potentially this occurs due to higher crosslink density around CB structures in the IR compounds or potentially due to its higher susceptibility to thermal oxidation, which might make the compound more prone to higher radical generation through double bound chain scission instead of single bond chain scission of carbon–carbon bonds. The thermal oxidation mechanism is not evident through $(M_N)_{\%diff}$ value, however a decrease of the ATR signal at around 1400 cm^{-1} which corresponds to the "bending vibration of C–H in the $=CH_2$ group of 3,4- or 1,2-unit" [18] can be observed in the supporting documentation, while comparing the Fourier Transform Infrared Spectroscopy (FTIR) signal of cured and smear wear layer samples of IRN220, where a reduction in the number of C=H bonds can be observed. The decomposition slope difference is also considerably higher for SBR9100GR which indicates both a greater amount of CB and also the most significant amount of chain scission due to its higher specific surface area filler. Finally, there appears to be no significant difference between compounds IRVN3 and SBRVN3.

Fujimoto et al. [19] discussed that an apparent increase in the oxygen content of the carbon black surface potentially results from the reaction of the Sulphur-Accelerator-ZnO system during pyrolysis, however in this investigation, an increase in the decomposition rate was only observed in smear wear layer samples and not in cured rubber samples. Therefore the increase in the decomposition rate most

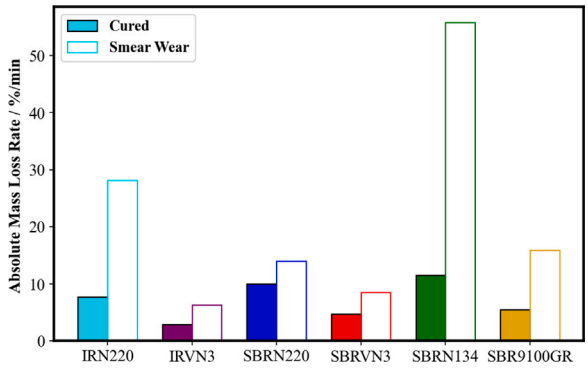

Fig. 8. TGA slope during the isothermal decomposition in air at 800 °C over a time for cured rubber and smear wear layer samples.

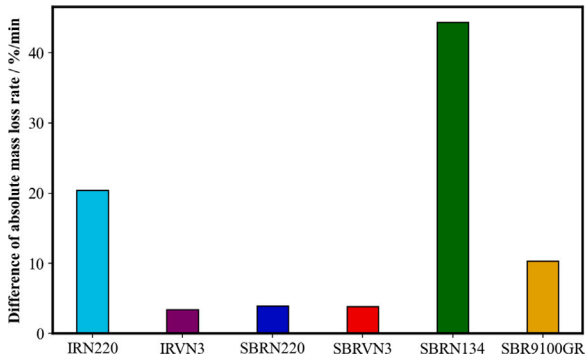

Fig. 9. TGA slope difference between cured rubber and smear wear layer samples during the isothermal decomposition in air at 800 °C.

probably results from an increase in the oxygen content due to the steps of chain scission and oxidation of polymer chains during abrasion and radical generation. This process is followed by oxidised low molecular weight polymer radicals being bonded or absorbed onto the available sites of the carbon black surface. When the oxidised low molecular weight polymer decomposes in nitrogen, a significant amount of oxygen is left on the CB surface which results in a more rapid decomposition in air. This is also confirmed by Koliolios et al. [20] and Wu et al. [9], where a higher oxygen content and higher amount of oxidation products were observed in smear wear layer samples.

3.3. Investigation smear wear particle structure through its dynamic mechanical properties

3.3.1. Effect of polymer and filler choice to smear wear particle properties and microstructure

Dynamic mechanical analysis was performed using temperature sweeps, where the tanδ of cured rubber samples, uncured rubber samples and fresh smear wear layer samples were plotted against temperature as shown in Figs. 10(a), 10(b) and 10(c) respectively.

Fig. 10(c) reveals a rather unexpected phenomenon, which is a peak in tanδ can be observed in all of the smear wear layer samples. This phenomenon was not observed in the cured and the uncured samples as shown in Figs. 10(a) and 10(b) respectively. According to Robertson and Rackaitis [12] this peak results from free polymer being present in the smear wear particle structure. This has also been confirmed by Wu et al. [9], using double quantum nuclear magnetic resonance measurements. An important observation being, that the silica filled compounds have a larger peak value compared to the CB filled compounds. Assuming that the structure of smear wear particles is similar to the schematic presented in Fig. 11, a higher tanδ peak is generated by the larger free polymer content [11,12]. Consequently, the silica filled compounds contain a significantly higher amount of free polymer, compared to the carbon black filled compounds. This occurs due to polymer-filler interface being less reactive, resulting in a significant amount of unreinforced polymer, detached from either the silica particles or the coupling agent. In the case of the CB filled compounds, polymer-filler interface damage is recoverable, which results in a lower free polymer content. Additionally, the compounds which presented a higher TGA slope difference between cured and smear wear layer samples, namely IRN220, SBRN134 and SBR9100GR, also have relatively lower tanδ peaks compared to the samples that have lower slope difference, namely IRVN3, SBRN220 and SBRVN3. Alongside with the $(M_N)_{\%diff}$ observation, this implies firstly that SBRN220, IRVN3 and SBRVN3 contain a greater amount of free polymer, compared to their other CB and silica filled counterparts, which is also potentially decrosslinked and has not attached to carbon black sites. Secondly, for the case of SBRN134 and SBR9100GR a large amount of free radicals are generated which effectively attach to CB sites and have a lower free polymer content compared to their other CB and silica filled counterparts respectively. Finally, that IRN220 has both a low amount of decrosslinked polymer and low amount of free polymer as the radicals generated during abrasion are more efficiently attached to the CB surface. Finally, the temperature at which the peak occurred is potentially influenced by the glass transition temperature of the rubber compounds. IR compounds as well as the smear wear particles they generate have a significantly lower temperature compared to SBR compounds and their generated smear wear particles respectively [9]. As a result the peak occurred at a lower temperature for the IR compounds and at a higher temperature for the SBR compounds.

3.3.2. Effect of ageing to smear wear particle properties and microstructure: Influence of filler colloidal properties

In bulk rubber it is anticipated that the higher surface area per gram fillers have higher Storage Modulus (SM) and Loss Modulus (LM) values as discussed in literature [17,21,22], however this trend does not translate to the smear wear particles as observed in Figs. 12(a) and 12(b). Both the SM and LM for SBRN220 and SBRVN3 are significantly larger than their higher specific surface area filled counterparts, SBRN134 and SBR9100GR. This further confirms that polymer-filler interface damage occurs and that it was also more significant for the higher specific surface area fillers. Potentially, this damage at the polymer-filler interface might be a key mechanism in the formation of smear wear, that relates to chain scission and stress concentration within the polymer-filler network.

Further information regarding filler damage and network recovery can be obtained by examining the effect of 24 h ageing on the dynamic mechanical properties of smear. It is evident that both the SM and LM of SBRN220 and SBRN134 significantly increased after ageing, the same behaviour was followed by SBR91000GR, whereas SBRVN3's properties appeared to reduce. To quantify this amplification or degradation effect stemming from ageing, the SM and LM values of the aged samples were divided by the values of the fresh smear samples, to obtain a ratio which is plotted against oscillation strain in Figs. 12(c) and 12(d) respectively.

The amplification ratio for both SM and LM appears to broadly give the same value for the different oscillation strains measured during the strain sweep. SBRN134 and SBRN220 have significantly higher amplification ratio compared to SBRVN3 and SBR9100GR, since the carbon black network effectively recovers with dwell time. Additionally, SBRN134 amplification ratio is larger compared to that of SBRN220, which could potentially imply that further ageing might result in SBRN134 SM and LM being higher than the SBRN220 smear, as expected in the original bulk rubber. The silica filler network however is not expected to recover as the nature of the polymer-filler interaction is a completely different chemical process. SBR91000GR has an amplification ratio which is larger than 1, potentially due to the high percentage of carbon black found in SBR9100GR as observed from

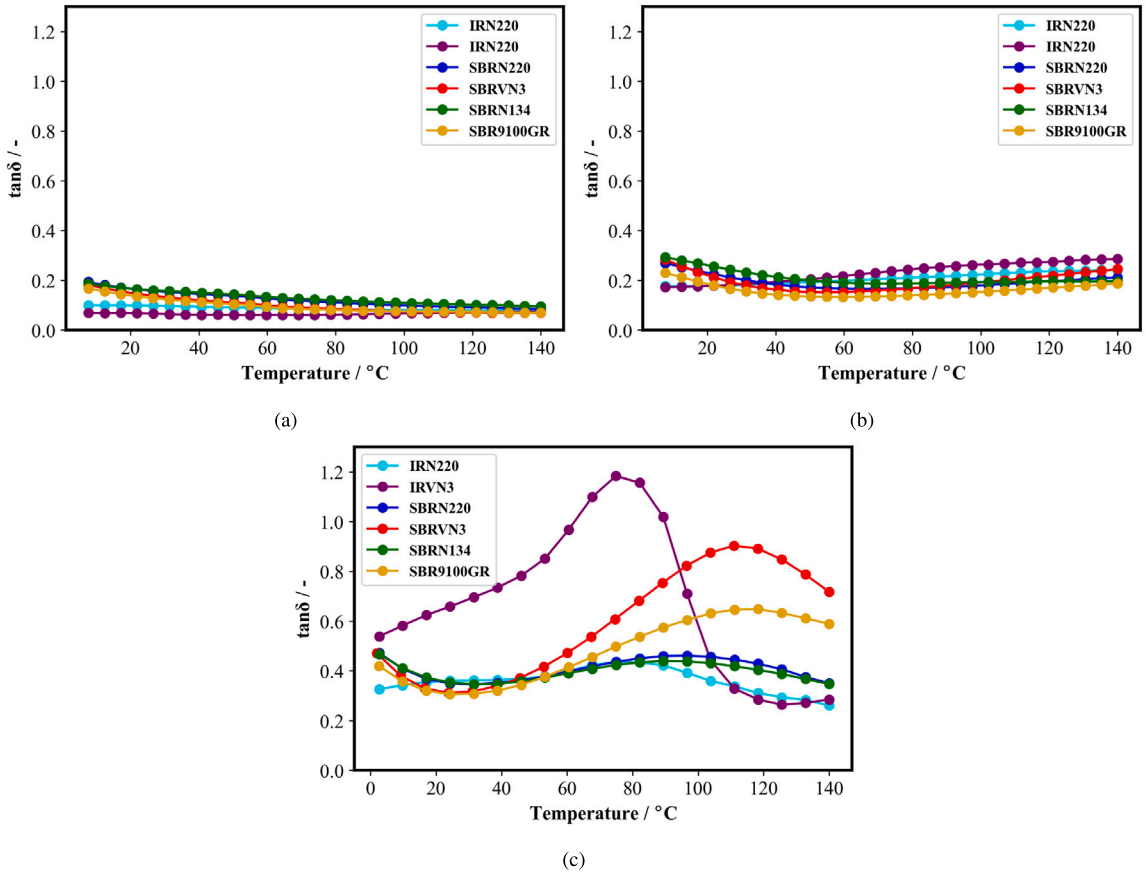

Fig. 10. tanδ over temperature for (a) cured rubber samples, (b) uncured rubber samples and (c) fresh smear wear samples.

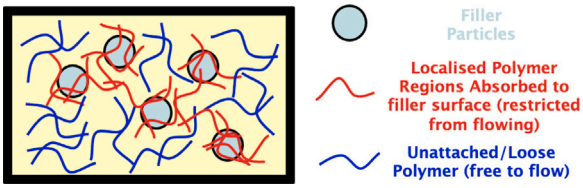

Fig. 11. Fresh Smear Wear Particle Microstructure Schematic.
Source: Adapted from Robertson and Rackaitis's [12]

Table 4, or due to the larger amount of polymer attaching to the CB surface. SBRVN3 not only did not recover after ageing, but there was also a degradation effect causing both SM and LM to have a lower value in the aged specimen. Understanding also the effect of smear wear particle ageing to the temperature dependent tanδ of smear wear layer samples can also provide crucial information regarding the ageing mechanisms concerning the free polymer. Fig. 13 shows that the tanδ peak appears to significantly reduce after ageing. This implies that the free polymer has started to reduce due to additional crosslinking from oxidation, as the decrease in the tanδ peak is more significant for the silica filled compounds, which also had the highest free polymer content. This mechanism would also explain the change in solubility observed by Wu et al. [8,9]. Not only does the CB network recover, but also the polymer network starts rapidly recovering through crosslinking initiated by oxidation for both IR [23] and SBR compounds [24].

Therefore, the proposed smear wear particle microstructure after ageing is presented in Fig. 14. Compared to the fresh microstructure presented in Fig. 11, during ageing crosslinks are introduced into the microstructure through oxidation, which reduce the mobility of the loose polymer chains. However, the effect that IR and SBR have on the polymer crosslinking mechanism and CB network recovery should be investigated to confirm these proposed mechanisms.

3.3.3. *Effect of ageing to smear wear particle properties and microstructure: Influence of polymer*

Similar to the filler effect on smear wear particle ageing mechanism investigation, the SM and LM of fresh and aged smear wear layer samples are presented in Figs. 15(a) and 15(b) and the respective ageing ratios are found in Figs. 15(c) and 15(d). It is evident that there are two competing mechanisms related to the recovery of the smear wear particle properties. The first one being thermal oxidation crosslinking which results in the degradation which is evident in both silica filled IR and SBR compounds and the second one is CB network recovery and potentially filler flocculation. Both SM and LM ageing ratios are higher for the SBR compounds compared to those for the IR compounds as seen in Figs. 15(c) and 15(d), potentially due to IR being more susceptible to thermal oxidation which results in crosslinking or decomposition as previously stated. This can also be seen from Fig. 16, where the tanδ of the IR compounds appears to reduce significantly compared to the tanδ of the SBR compounds after ageing.

To study the ageing effect the smear wear layer samples were aged for a month and a new SM and LM ageing ratio was obtained by dividing the moduli obtained from the 1 month aged samples by the moduli obtained from the fresh samples as presented in Figs. 17(a) and 17(b) respectively. It appears that after 1 month of ageing the mechanisms are dominated by the polymer instead of the filler in contrast to what was observed in the 1 day ageing comparison. After 1 month the SBR compounds have started to lose their mechanical properties whereas the IR samples appear to have greater reinforcement potentially due to high crosslinking efficiency during oxidation due to the possible oxidation mechanisms for polyisoprene as proposed by

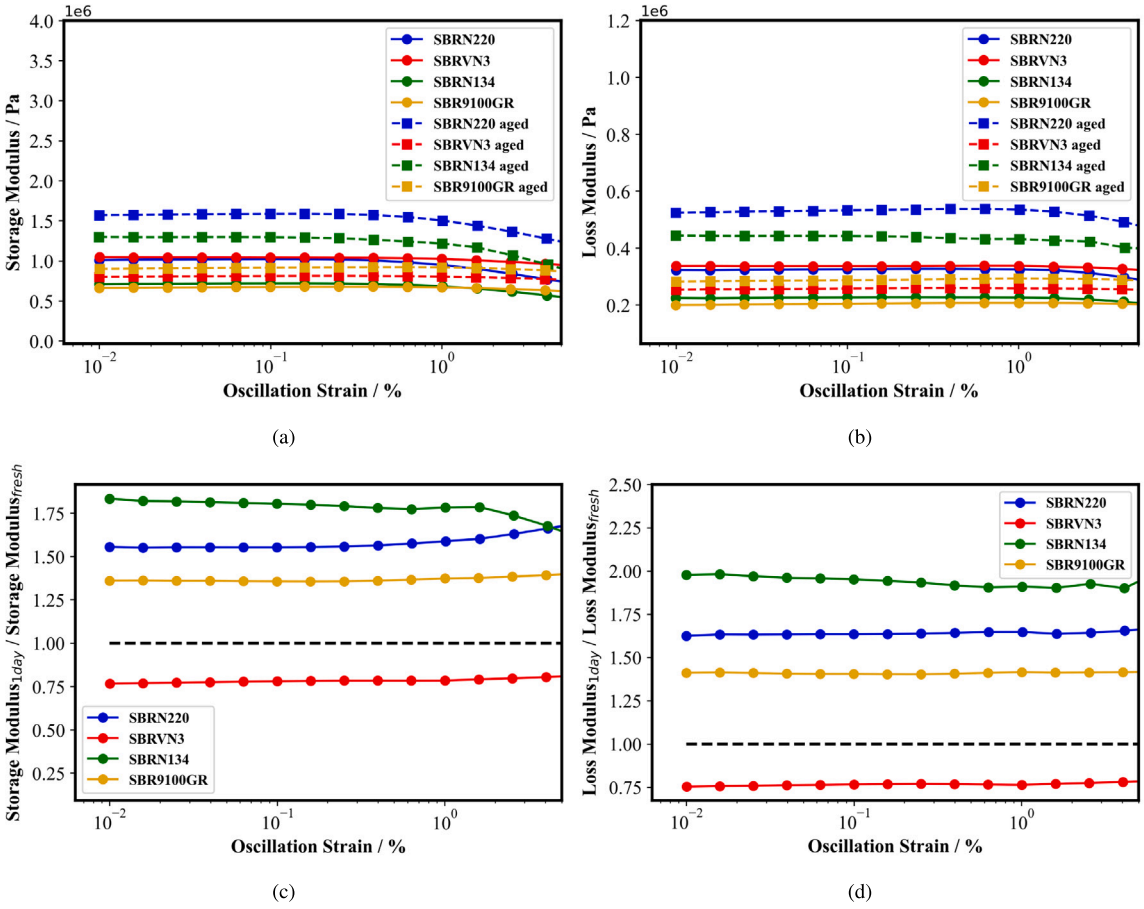

Fig. 12. Storage Modulus (a), Loss Modulus (b) and their respective reinforcement ratios (c), (d) of fresh and 1 day aged smear wear particles for filler type comparison purposes.

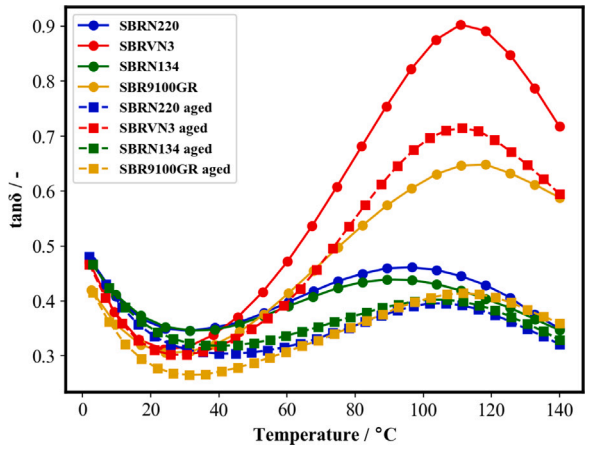

Fig. 13. tanδ over temperature for fresh and 1 day aged smear wear layer samples.

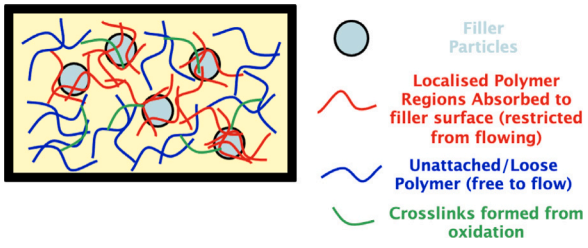

Fig. 14. Aged Smear Wear Particle Microstructure Schematic.

Colin et al. [23] and for SBR as proposed by Guo et al. [24]. This observation suggests that the CB network recovery occurs more rapidly than the polymer crosslinking and recombination during oxidation.

3.4. SEM results

To confirm polymer-filler interface damage, SEM images were obtained for the smear layers generated. Although this task was extremely challenging, a polymer-filler interface was effectively captured for the smear wear particles of SBRN134 as observed in Fig. 18. From Fig. 18, it is evident that there is phase separation between carbon black particles and the polymer. This observation explains the weaker mechanical properties of smear compared to bulk rubber and could pose the question whether the dispersion of the filler is also affected during abrasion which could also further explain the difference in the mechanical properties of smear generated by compounds with different fillers as well as their dynamic mechanical properties. Finally, the structure which was proposed after observing the second relaxation of smear wear layer samples is further confirmed in Fig. 18, as two polymer phases appear to be present in smear wear particles as previously discussed.

4. Conclusion

This research investigated the smear wear particles produced by six different tyre tread compounds using blade abrasion, to elucidate their microstructure and their formation and ageing mechanisms. It was found that the number average molecular weight of smear wear particles was significantly smaller compared to that of the uncured rubber chains and also that the amount of chain scission could be potentially quantified by observing the percentage difference of the

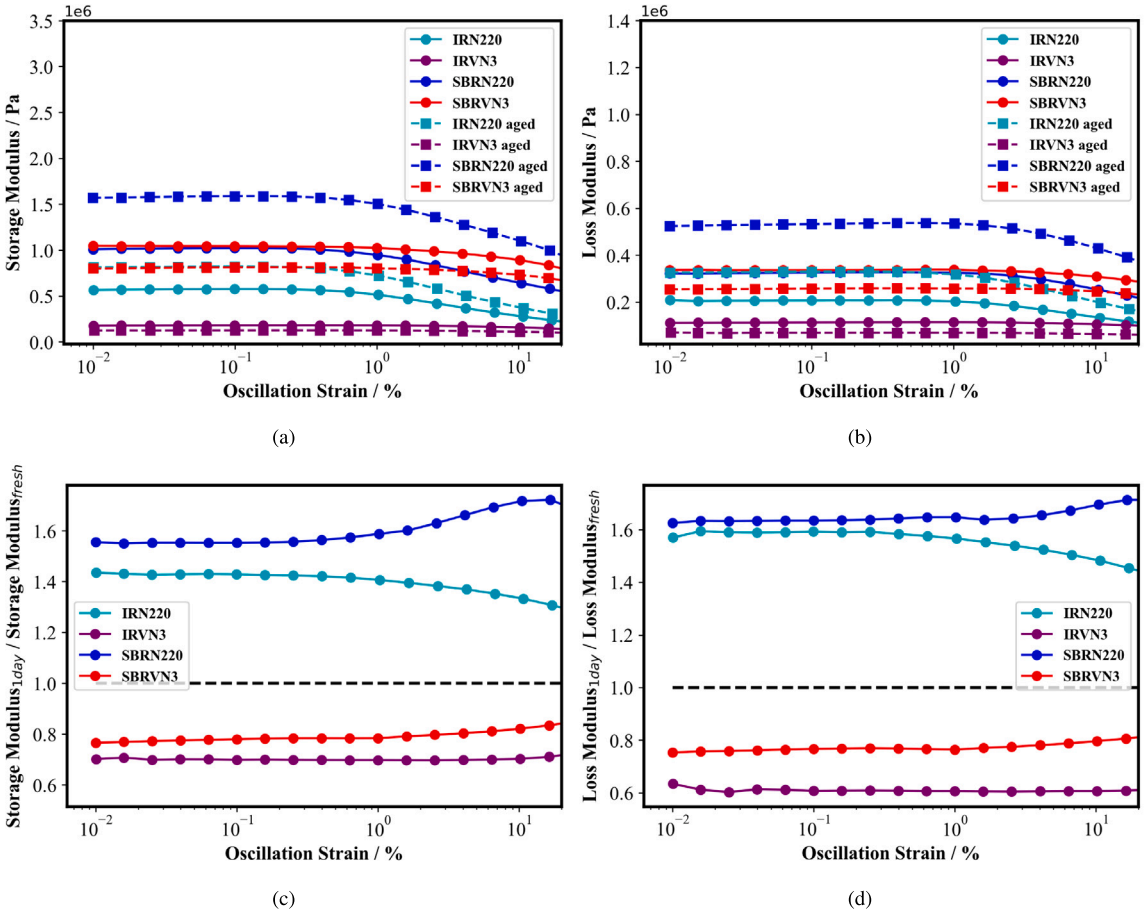

Fig. 15. Storage Modulus (a), Loss Modulus (b) and their respective reinforcement ratios (c), (d) of fresh and 1 day aged smear wear particles for polymer type comparison purposes.

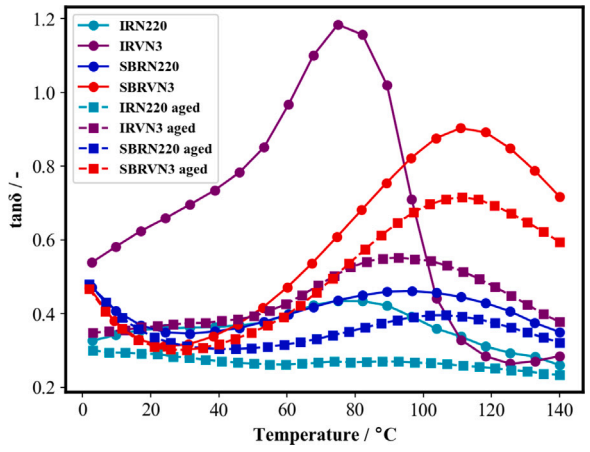

Fig. 16. tanδ over temperature for fresh and 1 day aged smear wear layer samples.

number average molecular weight. The smear wear particle content was investigated through TGA and it was found that the CB content appears to increases in the higher specific surface area filled SBR compounds, potentially due to a larger amount of radicals being generated during abrasion which then attach to CB surface. This theory was tested by investigating the isothermal decomposition of smear wear particles in air and comparing it with that of the cured rubber samples and it was observed that smear wear particles from all samples decompose more quickly. This potentially occurs due to oxidised low molecular weight polymer chains attaching to CB surface during smear wear layer formation, which in turn decompose in nitrogen, without removing the additional oxygen amount on the CB surface, resulting in a faster decomposition after the TGA run was switched to air. Finally, the smear wear particle structure was investigated using dynamic mechanical analysis. A second peak in tanδ was observed which was attributed to an amount of loose decrosslinked polymer being present in smear wear particles as it has been indicated previously [9,11,12]. This suggests that there are two different polymer phases in smear wear particles, one localised and bound to filler particles and one free to flow, as also observed from SEM.

The smear wear particle microstructures of the six different compound formulations can be divided into three different groupings as shown in Fig. 19. Group 1 includes IRVN3 and SBRVN3 where the highest tanδ is observed, which implies a higher amount of free polymer content and lower amount of restricted polymer content. Group 2 consist only of SBR9100GR where intermediate tanδ is observed, which implies a intermediate amount of free polymer content and intermediate amount of restricted polymer content. Finally, Group 3 includes the CB filled compounds IRN220, SBRN220 and SBRN134 where the lowest tanδ is observed, which implies a lower amount of free polymer content and higher amount of restricted polymer content. Through this grouping approach, tyre tread compound formulations could be designed to optimise the amount of free or restricted polymer content as well as the tanδ of any smear wear particles generated during tyre tread abrasion. This helps to understand the effect of different smear wear particle microstructures on crucial factors of tyre tread performance including wear rate and grip.

The amount of free to flow, decrosslinked polymer was found to significantly reduce after ageing, resulting in a reduction in tanδ peak.

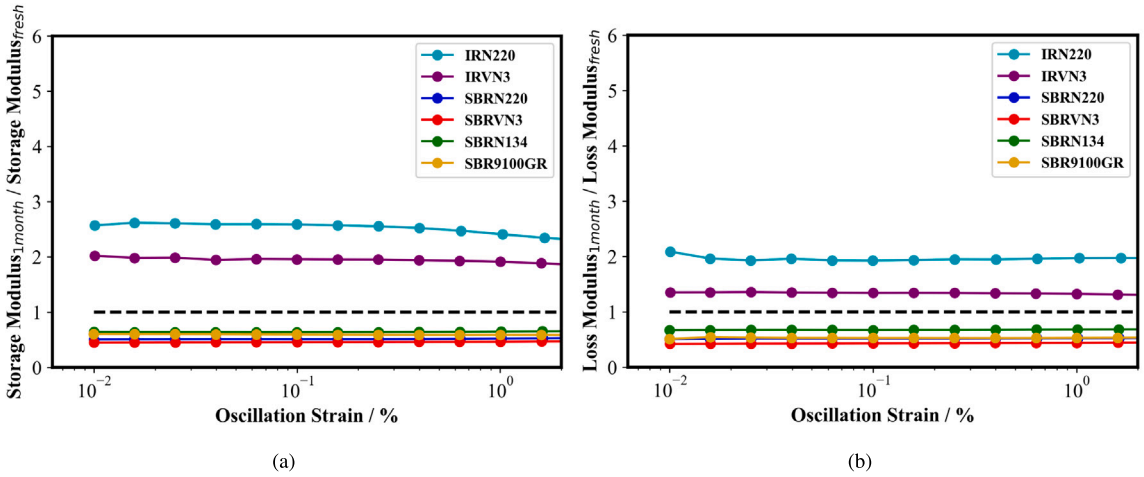

Fig. 17. 1 month ageing reinforcement amplification ratio of (a) storage and (b) loss moduli of smear wear particles.

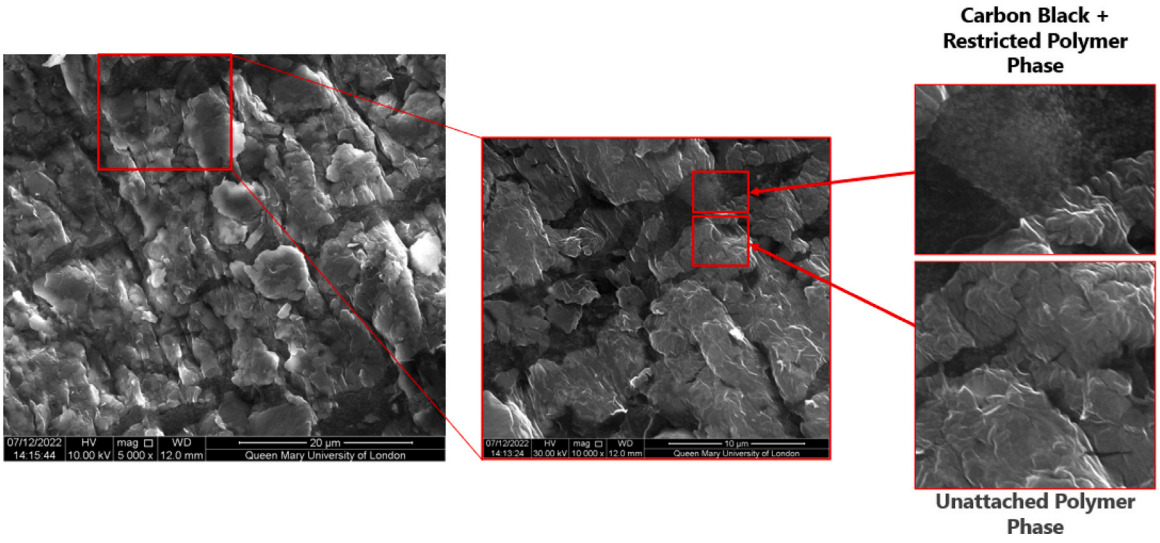

Fig. 18. SEM image of SBRN134 smear wear layer sample.

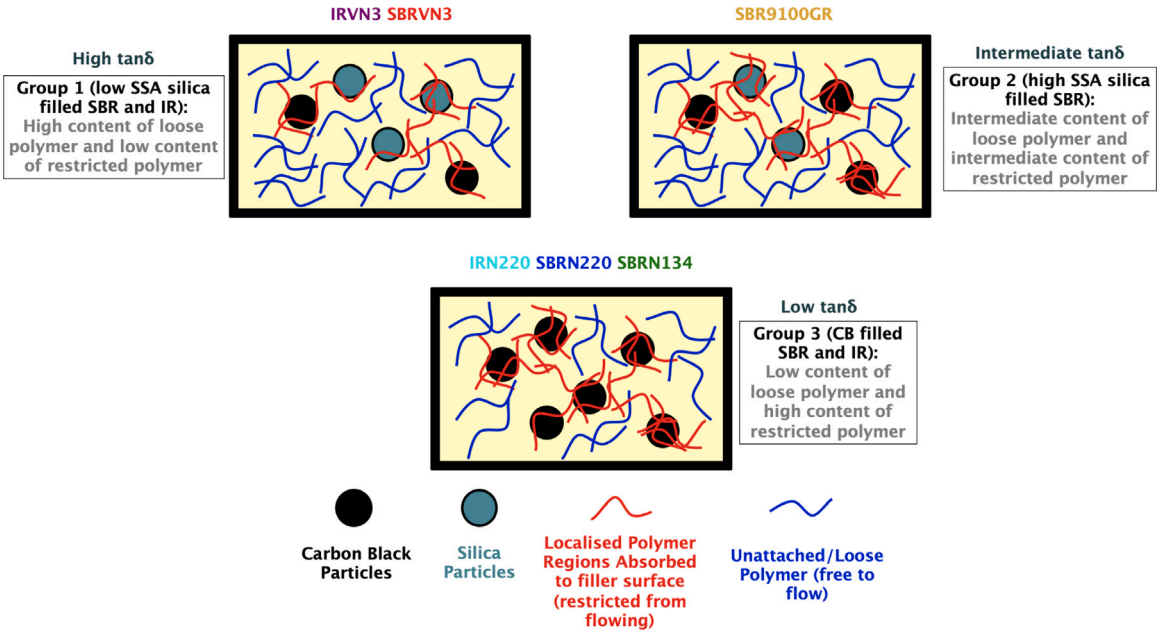

Fig. 19. Summary and grouping of fresh smear wear particle microstructure produced from different compound formulations.

Additionally, it is also proposed here for the first time that two different mechanisms are observed in the smear wear particle structure, one involving crosslinking and polymer recombination due to oxidation and one involving the recovery of the carbon black network. Finally, it was found that the ageing mechanisms after 1 day were dominated by the filler type and surface area and thus the CB network recovery and after 1 month they were dominated by the polymer and thus crosslinking oxidation of polymer chains.

Further research could potentially involve a solubility study to evaluate the loose and bound polymer content in smear wear particles and how it varies between different compounds. The oxidative reactions occurring during smear wear particle formation could also be studied through electron paramagnetic resonance or potentially through a nuclear magnetic resonance technique. Finally, smear wear layer samples could be aged in an inert atmosphere to understand and deconvolute the two ageing mechanisms which influence the polymer and filler network recovery in smear wear particles.

CRediT authorship contribution statement

E. Koliolios: Writing – original draft, Visualization, Investigation, Data curation. **S. Nakano:** Writing – review & editing, Supervision, Project administration, Funding acquisition, Conceptualization. **T. Kawamura:** Writing – review & editing, Supervision, Conceptualization. **J.J.C. Busfield:** Writing – review & editing, Supervision, Resources, Project administration, Methodology, Funding acquisition, Conceptualization.

Declaration of competing interest

The authors declare the following financial interests/personal relationships which may be considered as potential competing interests: Evangelos Koliolios reports equipment, drugs, or supplies was provided by Sumitomo Rubber Industries Ltd. If there are other authors, they declare that they have no known competing financial interests or personal relationships that could have appeared to influence the work reported in this paper.

Data availability

Data will be made available on request.

Acknowledgements

Evangelos Koliolios would like to thank Sumitomo Rubber Industries, Ltd for funding his studies and the Soft Matter Group at Queen Mary University of London for their continuous support. The authors would also like to thank William Kyei-Manu for proofreading this paper and providing feedback.

Appendix A. Supplementary data

Supplementary material related to this article can be found online at https://doi.org/10.1016/j.polymer.2024.126982.

References

[1] D.H. Champ, E. Southern, A.G. Thomas, Advances in Polymer Friction and Wear, Springer US, 1974, pp. 133–144.
[2] E. Southern, A.G. Thomas, Studies of rubber abrasion, Rubber Chem. Technol. 52 (1979) 1008–1018.
[3] A.N. Gent, C.T.R. Pulford, Mechanisms of rubber abrasion, J. Appl. Polym. Sci. 28 (1983) 943–960.
[4] H. Liang, Y. Fukahori, A.G. Thomas, J.J.C. Busfield, Rubber abrasion at steady state, Wear 266 (2009) 288–296.
[5] H. Liang, Y. Fukahori, A.G. Thomas, J.J.C. Busfield, The steady state abrasion of rubber: Why are the weakest rubber compounds so good in abrasion? Wear 268 (2010) 756–762.
[6] A. Ahagon, Chemical aspect of rubber abrasion, Nippon Gomu Kyokaishi 79 (2006) 500–506.
[7] S. Nakano, Y. Yamahashi, F. Kaneko, T. Zushi, T. Mabuchi, T. Kawamura, T. Tada, Effect of molecular structure on the mechanochemical wear behavior of hydrogenated and conventional sbr rubbers, KGK Kautschuk Gummi Kunststoffe 74 (2021) 56–61.
[8] G. Wu, The Mechanisms of Rubber Abrasion, Queen Mary University of London, London, 2016.
[9] G. Wu, P. Sotta, M. Huang, L.B. Tunnicliffe, J.J. Busfield, Characterisation of sticky debris generated during smear wear, Rubber Chem. Technol. 96 (4) (2023) 588–607.
[10] M. Huang, M. Guibert, J. Thévenet, C. Fayolle, T. Chaussée, L. Guy, L. Vanel, J.-L. Loubet, P. Sotta, A new test method to simulate low-severity wear conditions experienced by rubber tire materials, Wear 410–411 (2018) 72–82.
[11] G. Tsagaropoulos, A. Eisenberg, Dynamic mechanical study of the factors affecting the two glass transition behavior of filled polymers. Similarities and differences with random ionomers, Macromolecules 28 (1995) 6067–6077.
[12] C.G. Robertson, M. Rackaitis, Further consideration of viscoelastic two glass transition behavior of nanoparticle-filled polymers, Macromolecules 44 (2011) 1177–1181.
[13] J.T. Gruver, K.W. Rollmann, Antioxidant properties of carbon black in unsaturated elastomers. Studies with cis-polybutadiene, J. Appl. Polym. Sci. 8 (1964) 1169–1183.
[14] E.M. Bevilacqua, Carbon black as an elastomer antioxidant. I. Effect of vulcanizing systems in SBR, J. Polym. Sci. B Polym. Lett. 5 (1967) 1109–1118.
[15] C.G. Robertson, N.J. Hardman, Nature of carbon black reinforcement of rubber: Perspective on the original polymer nanocomposite, Polymers 13 (4) (2021) 538.
[16] P.K. Pal, A.K. Bhowmick, S.K. De, The effects of carbon black-vulcanization system interactions on natural rubber network structures and properties, Rubber Chem. Technol. 55 (1982) 23–40.
[17] S.M. Hosseini, M. Razzaghi-Kashani, Catalytic and networking effects of carbon black on the kinetics and conversion of sulfur vulcanization in styrene butadiene rubber, Soft Matter 14 45 (2018) 9194–9208.
[18] D. Chen, H. Shao, W. Yao, B. chen Huang, Fourier transform infrared spectral analysis of polyisoprene of a different microstructure, Int. J. Polym. Sci. 2013 (2013) 1–5.
[19] K. Fujimoto, T. Miyajima, S. Kijima, Study on char black recovered from scrap tires by pyrolysis (I) properties of char recovered from scrap tires by pyrolysis, Nippon Gomu Kyokaishi 51 (12) (1978) 938–948.
[20] E. Koliolios, S. Nakano, T. Kawamura, I. Tsumori, J. Busfield, Constitutive Models for Rubber XII, Taylor & Francis Group, 2022, pp. 483–488.
[21] W.A. Kyei-Manu, C.R. Herd, M. Chowdhury, J.J.C. Busfield, L.B. Tunnicliffe, The influence of colloidal properties of carbon black on static and dynamic mechanical properties of natural rubber, Polymers 14 (6) (2022) 1194.
[22] K.J. Rutherford, K. Akutagawa, J.L. Ramier, L.B. Tunnicliffe, J.J.C. Busfield, The influence of carbon black colloidal properties on the parameters of the Kraus model, Polymers 15 (7) (2023) 1675.
[23] X. Colin, L. Audouin, J. Verdu, Kinetic modelling of the thermal oxidation of polyisoprene elastomers. Part 1: Unvulcanized unstabilized polyisoprene, Polym. Degrad. Stab. 92 (2007) 886–897.
[24] L. Guo, G. Huang, J. Zheng, et al., Thermal oxidative degradation of styrene-butadiene rubber (SBR) studied by 2D correlation analysis and kinetic analysis, J. Therm. Anal. Calorim. 115 (2014) 647–657.